Applied Mathematics & Information Sciences
An International Journal

http://dx.doi.org/10.12785/amis/091L06

Mechanics of Energy Absorption by Progressive Plastic Deformation of a Square Column with an Ellipsoidal Bulge Base

M. A. Hassan[2,3,*], *Amir Radzi Ab. Ghani*[1], *Zahari Taha*[4] *and M. A. Hamdi*[2]

[1] Faculty of Mechanical Engineering, Universiti Teknologi MARA, 40450 Shah Alam, Selangor, Malaysia
[2] Department of Mechanical Engineering, Faculty of Engineering, University of Malaya, 50603 Kuala Lumpur, Malaysia
[3] Department of Mechanical Engineering, Faculty of Engineering, Assiut University, 71516 Assiut, Egypt
[4] Faculty of Manufacturing Engineering, Universiti Malaysia Pahang, 26300 Kuantan, Pahang, Malaysia

Received: 7 Nov. 2013, Revised: 8 Mar. 2014, Accepted: 9 Mar. 2014
Published online: 1 Feb. 2015

Abstract: : Thin-walled square columns are generally used as energy absorber in various applications due to their ease of fabrication and installation, high energy absorption capacity in terms of progressive plastic deformation and long stroke. However, the main drawback of a standard square column is the high initial peak force. An ellipsoidal bulge base is proposed to overcome this shortcoming and at the same time to improve the crush performance. Static axial crushing were performed by finite element analysis to determine the initial peak force (IPF), crush force efficiency (CFE) and plastic specific energy absorption (SEA) of columns having ellipsoidal bulge bases with various thicknesses. It was found that the bulge base significantly enhanced the column crush performance as well as the deformation characteristics. A comparison with the plain square column was carried out and it was found that the bulge base reduced the initial peak force and increased the crush force efficiency. A simple analytical approach is proposed to predict the reduction of initial peak force with the use of this trigger mechanism.

Keywords: crush response, energy absorption, progressive failure, square column, finite element analysis

1 Introduction

Energy absorbers in the form of columns and frusta of various shapes and sizes are mainly employed for vehicle impact protection during collision and they have been extensively studied for the past five decades [1,2]. Ductile materials such as steels and aluminium are the preferred choice as they exhibit large plastic deformation before total fracture. These materials absorb the excessive kinetic energy during impact by various mechanisms such as friction, fracture, shearing, bending, tension, crushing and plastic deformation.

Vast reviews of tube type and collapsible energy absorbers have been presented by A.G. Olabi et al. [3] and Alghamdi [4]. The works highlight the different modes of deformation and outline the theoretical, numerical and experimental methods to understand the response of devices subjected to a range of loading conditions. Square and circular columns are the most commonly utilised shapes and form the foundation for most experimental, numerical and analytical work.

Alexander [5] initially developed the analytical model to determine the mean load of an axially compressed circular tube. A kinematically admissible deformation mode was assumed based on experimental observations. The internal energy absorbed by bending and stretching at and between the joints of the complete fold was equated to the external work done to deform the tube. Similiarly Mamalis [6] utilized the same technique to determine the energy absorbed and mean post-buckling loads of thin-walled frusta. An analytical model to predict the response of a tapered thin-walled cylindrical tube under axial loading was developed by Chirwa [7]. Energy dissipation was due to tube bending, circumferential stretching, buckling and friction between the tube and dies.

An analytical model of a square column subjected to axial crushing was developed by Wierzbicki and

* Corresponding author e-mail: mohsenegypt@um.edu.my

Abramovicz [8]. By considering the kinematically admissible crushing mechanism and equating the plastic energy dissipation to the external work done, the force-displacement response and mean crushing force were obtained. Based on experimental results, Abramovicz and Jones [9,10] further refined the model by including the effect of strain rate sensitivity and effective crushing distance.

Despite the superior impact performance of tubular structures, major drawback is the high initial peak force with potential to cause severe damage. Therefore, the necessity for further structure optimization has prompted researchers to experiment with new geometries, configurations and material combinations. Zhang and Chang [11] carried out comparative studies of energy absorption characteristics of foam filled and multi cell columns, both which exhibit higher energy absorption than plain columns. However, the additional stiffness resulted in high initial peak force. A trigger mechanism in the form of a groove was incorporated in the column to reduce the high initial peak force while maintaining the energy absorption performance. Daneshi and Hosseinipou [12] experimented work on grooved thin-walled tubes subjected to axial compression. The function of the groove in the tube is to force plastic deformation to occur at predetermined intervals along the tube. The results showed favourable characteristics with the grooved tubes exhibiting lower initial peak forces and more uniform, stable crushing modes and mean forces.

In a numerical study, Zhang et al. [13] looked into a new tube configuration the retractable/telescopic tube, whereby; straight retractable (SR) and tapered retractable (TR) tubes were subjected to axial crushing. The inversion process of the proposed tubes under axial crushing was simulated using the non-linear finite element code LS-DYNA. The results showed that the proposed tubes had lower peak force as well as higher crush force efficiency (CFE) and specific total efficiency (STE). Zhang et al. [14] studied the influence of a buckling initiator on the response of an axially crushed square tube. The buckling initiator consisted of a pre-hit column with pulling strips attached to both sides of the inner tube near the impacted end. A significant decrease in initial peak force was evident, while little influence was noted on the mean force and deformation mode. Added advantages of this system are that the stiffness of the intact square tube in its normal structural function is maintained and a more stable and uniform crushing mode is ensured. A simplified analytical model to relate the reduction of initial peak load with the geometric imperfection was developed. The model was able to predict the effectiveness of the buckling initiator to a certain extent.

Zhang et al. [15] also extended the use of this buckling initiator to circular aluminium tubes subjected to dynamic axial loading. The effect of different numbers of pulling strips, pre-hit heights and inclination angles of the pulling strips on the initial peak force and mean crushing force were experimentally studied. With a suitable pre-hit height selection, the initial peak force was reduced by 30%. A simplified theoretical model to explain the initial peak force reduction and energy dissipation mechanisms was developed. The model and experimental results were in good accord. Yamashita et al. [16] studied dynamic axial crushing of an aluminium tubular structure with a hat-shaped configuration. A buckling initiator consisting of two solid blocks attached to the side wall at a specified height of the structure was used to initiate the first plastic buckling lobe. The solid blocks provided inertia force that caused wall bending.

Current research studies explore the incorporation of trigger mechanisms into structures with the aim to induce failure in a desired manner and produce impact responses that are optimized for a wide range of conditions. This present study focuses on the crush behavior and progressive deformation of square column with an ellipsoidal bulge base as the trigger mechanism. Crush performance indices facilitate the evaluation of the proposed mechanisms efficiency. The crush performance of plain square column and column with a proposed ellipsoidal bulge base is assessed through numerical simulation under static axial loading. A simplified analytical model is proposed to describe the energy absorption mechanism and explain the reduction of initial of peak force with the use of this trigger mechanism.

2 Proposed Trigger Mechanism

In the present study, an ellipsoidal bulge base is added to a plain square column as a trigger mechanism to enhance the crush performance. The basis for this design is that the stress from the bulge base forming induces initial stress on the column during flattening of the bulge base. This initial stress will facilitate buckling of the column sides and reduce the initial peak force. The design configurations and dimensions are provided in Figure 1 and Table 1. Bulge base thickness, t_2 will be varied to investigate its effect on the initial peak force of the column.

3 Finite Element Modelling

The plain square column was modeled in ABAQUS as a 3D deformable shell. The bottom plate, which represents the support, and the top plate, which represents the compression platen/impactor were modeled as discrete rigid bodies. Approximately 5000 and 1800 type S4R, 4-noded linear quadrilateral explicit shell elements were used for the column and the bulge base. The S4R elements have reduced integration and enhanced hourglass control. For the top and bottom plates, 8, type R3D4, 4-noded rigid linear quadrilateral elements were used. The die and punch were modeled as rigid surfaces

Table 1: Design dimensions

	Plain column	Column with ellipsoidal bulge base
Length, L(mm)	250	250
Width, W(mm)	50	50
Column thickness, t_1 (mm)	1.57	1.57
Ellipse diameter,ϕ (mm)	-	60
Ellipse thickness, t_2 (mm)	-	0.6,0.7, 0.8,0.9, 1
Ellipse height, H_1 (mm)	-	15

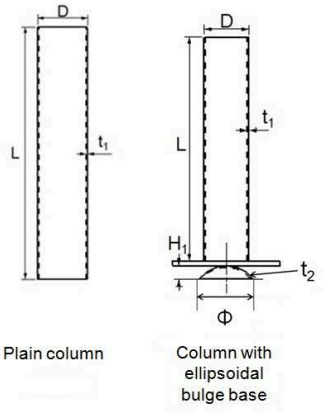

Fig. 1: Design configurations

and consisted of 400 and 800 discrete rigid R3D4 elements. Figure 2 shows the finite element assembly of the square column with an ellipsoidal bulge base.

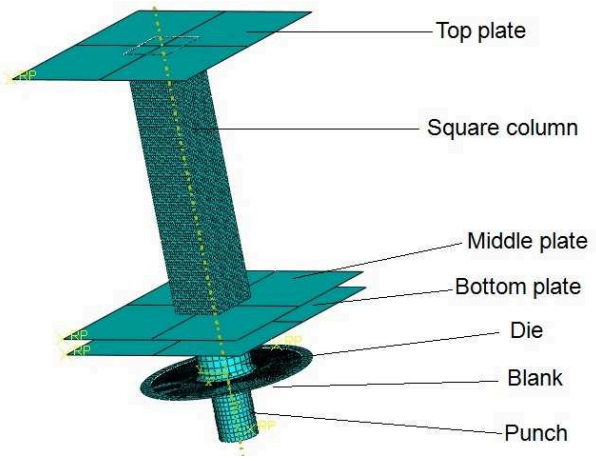

Fig. 2: Finite element assembly of a square column with an ellipsoidal bulge base

The column is made of aluminium 6063-T5. General material properties of the column are provided in Table 2, and the true stress-strain curve obtained from the uniaxial tensile test is shown in Figure 3. The material mechanical behavior can be safely described by the elastic-plastic linear strain hardening model.

[ht]

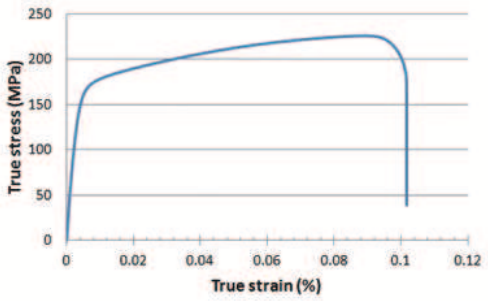

Fig. 3: Experimental true stress-strain curve for Aluminium 6063-T5

The ABAQUS/Explicit solver was employed to run the analysis. The contact behavior between all components was set up under the interaction module. The contact properties consisted of tangential behavior, having a penalty friction formulation with a coefficient of 0.25. The normal behavior used the hard contact formulation to allow the separation of bodies following contact. A general (explicit) contact was utilized where all contact surfaces including self contact were automatically identified by the system. In axial loading, the top plate was moved down by 70% of the column length to ensure maximum effective crushing. A suitable time scaling helped ensure that the effect of inertia is negligible for quasi-static loading. The boundary conditions for the top plate were V1=V2=VR1= VR2 = VR3=0, implying that the plate could only move in the vertical z-direction. The bottom plate was fully constrained. The columns bottom edges were restricted in the z-direction only. Column movement in the x- and y-direction was restrained by the friction between the column and the bottom plate. For the column with a bulge base, during forming of the blank, the holder was fully constrained while the blank was

Table 2: General properties of Aluminium 6063-T5

Density (kg/m^3)	Ultimate tensile strength (MPa)	Yield strength (MPa)	Youngs Modulus (GPa)	Poissons ratio
2700	220	180	65	0.3

constrained at its edge. The punch was then moved by 15 mm to produce the specified bulge height. Multi steps analysis were performed where results from previous analysis were used as inputs for the subsequent steps. The blank was first punched to produce the ellipsoidal bulge base. The ellipsoidal bulge base was then placed below the column and separated by a rigid middle plate. The bulge and the column were then compressed by the top plate.

4 Proposed Analytical Method

ellipsoidal bulge base consists of three steps. The first step is the forming or punching of the bulge base (see Figure 4). The flow stress at the end of the bulging process is calculated as follows:

The blank thickness after bulging using is determined using,

$$\frac{t_d}{t_o} = \frac{1}{1+(2h_d/d_c)^2} \tag{1}$$

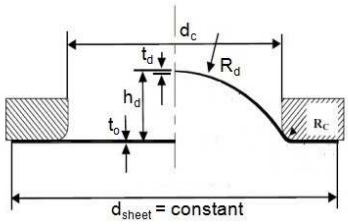

Fig. 4: Forming of the bulge base

To express (t_d/t_o) in terms of t_d, t_o, h_d and d_c, we use the expression that states that volume of the sheet metal remains constant before and after bulging.

$$\pi(\frac{d_c}{2})^2 t_o = \pi[(\frac{d_c}{2})^2 + h^2]t_d \tag{2}$$

Rearranging the above,

$$h_d = \frac{d_c}{2}\sqrt{\frac{t_o - t_d}{t_d}} \tag{3}$$

Expressing equation 1 as,

$$\frac{t_d}{t_o} = \frac{1}{1+\frac{4h_d h_d}{{d_c}^2}} \tag{4}$$

Substituting equation 3 into equation 4,

$$\frac{t_d}{t_o} = \frac{1}{1+\frac{2h_d}{d_c}\sqrt{\frac{t_o-t_d}{t_d}}} \tag{5}$$

From,

$$\varepsilon = \ln(\frac{t_d}{t_o}) \tag{6}$$

$$\sigma = K\varepsilon^n \tag{7}$$

Substituting equations 5 and 6 into equation 7,

$$\sigma = K[\ln(\frac{1}{1+\frac{2h_d}{d_c}\sqrt{\frac{t_o-t_d}{t_d}}})]^n \tag{8}$$

where,
t_o = thickness of sheet before bulging (m)
t_d = thickness of sheet after bulging (m)
d_c = diameter of bulge base (m)
h_d = height of bulge base (m)
K = strength coefficient (MPa)
n = strain hardening

The second step is the flattening of the bulge base. The flow stress from the forming of the bulge base will influence the force required to flatten the bulge base. From simulation and experiment, it can be seen that flattening of ellipsoidal bulge base resulted in circumferential wrinkles on the base. Figure 5 shows the formation of wrinkles during the bulge base flattening process. There are three circumferential wrinkles and one central hump (bulge). The wrinkles are assumed to be semi-circular in shape, have equal size and remain constant throughout the flattening process. The wrinkles are also assumed to travel from the centre of the base to their respective final positions and the distances between wrinkles are assumed to be the same for all wrinkles.

Cross sectional area of the half ellipse is given by,

$$A_{ellipse} = \pi t\sqrt{\frac{{h_d}^2 + (d_c/2)^2}{2}} \tag{9}$$

Cross sectional area of the flattened bulge base (with wrinkles) is given by,

$$A_{fbb} = [d_c - 7(2r_h) + 7(\pi r_h)]t \tag{10}$$

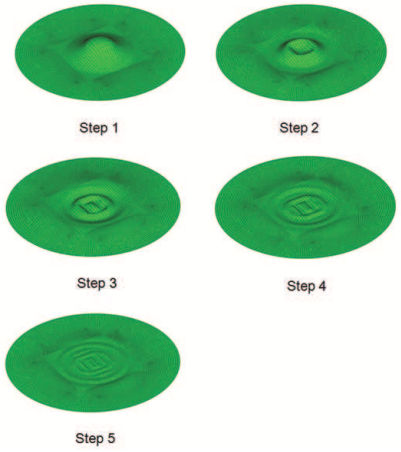

Fig. 5: Formation of circumferential wrinkles during the bulge base flattening process

For constant volume, cross sectional area of the half ellipse must be equaled to flattened bulge base,

$$A_{ellipse} = A_{fbb}\pi t\sqrt{\frac{h_d{}^2+(d_c/2)^2}{2}} = [d_c - 7(2r_h)+7(\pi r_h)]t \tag{11}$$

Hinge radius is therefore,

$$r_h = \frac{\pi\sqrt{\frac{h_d{}^2+(d_c/2)^2}{2}} - d_c}{7\pi - 14} \tag{12}$$

Distance between wrinkles is given by,

$$e = \frac{\pi\sqrt{\frac{h_d{}^2+(d_c/2)^2}{2}} - 7\pi r}{8} \tag{13}$$

Work done by the travelling hinges (wrinkles) moving from the centre of the bulge base to their final respective positions,

$$W_{th} = \frac{3M_o L_{th} S}{b} \tag{14}$$

Determining the length of each wrinkle (See Figure 6),

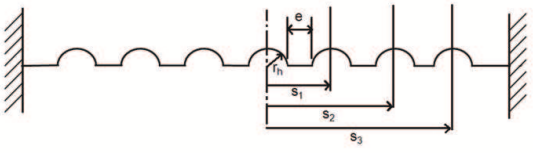

Fig. 6: Assumed bulge base wrinkle formation after flattening

$$L_{th} = 2\pi S L_{th1} = 2\pi S_1 L_{th2} = 2\pi S_2 L_{th3} = 2\pi S_3 \tag{15}$$

S_1, S_2 and S_3 are positions of each wrinkle from the centre of the bulge base.

$$s_1 = 2r_h + es_2 = 2s_1 s_3 = 3s_1 \tag{16}$$

Expressing S_1, S_2 and S_3 in term of h for the distance travelled by the wrinkles,

$$s_1 = \frac{2r_h + e}{d_c}.4h_d s_2 = 2s_1 s_3 = 3s_1 \tag{17}$$

Work done by the travelling hinges,

$$W_{th} = \frac{3M_o}{rh}[L_{th1}S_1 + L_{th2}S_2 + L_{th3}S_3] \tag{18}$$

Force by the travelling hinges (bulge base flattening force),

$$F_{bbf} = \frac{dW_{th}}{dh_d} = \frac{d\frac{3M_o}{rh}[L_{th1}S_1 + L_{th2}S_2 + L_{th3}S_3]}{dh_d} \tag{19}$$

given,
t_2 = thickness of bulge base (m)
r_h = hinge radius (m)
σ_o= yield stress (N/m^2)
e = distance between travelling hinges (m)
L_{th} = length of travelling hinges (m)
s = distance travelled by travelling hinges (m)
M_o= plastic bending moment per unit length (Nm/m)

The initial peak force of the column with a bulge base, $F_{IPF,cbb}$ is directly proportional to the bulge base flattening force, F_{bbf} . The higher the Fbbf, the higher the $F_{IPF,cbb}$. The bulge base flattening force is multiplied by a factor which is the ratio of column thickness to the bulge base thickness to give the predicted $F_{IPF,cbb}$. This ratio acts an amplification factor which increases the bulge base flattening force that reacts on the column to cause yielding and progressive buckling.

$$F_{IPF,cbb} = F_{bbf} X \frac{t_1}{t_2} \tag{20}$$

5 Result and discussion

5.1 Static responses

Figure 7 shows the static responses for the plain column and columns with different bulge base thicknesses. The plain column showed a sudden high initial peak force followed by lower fluctuating mean forces. All columns with bulge bases showed much lower initial peak forces compared to the plain column. Columns with bulge bases showed gradual increase in force until the initial peak

force. This was due to the flattening of the bulge base before progressive crushing of the column commenced. The column with a bulge base thickness of 0.6 mm showed a force displacement response that approached the ideal energy absorber where the value of the mean force is almost the same as the initial peak force. Figure 8 shows the failure modes for the plain column and columns with different bulge base thicknesses under static loading. All columns exhibited progressive crushing failure mode. The main differences were the size and shape of the folds. The plain column failed in Type I progressive buckling mode where the column faces were uniformly folded in a systematic manner. Columns with bulge bases failed in a combination of Type I and Type II buckling modes where the columns faces expanded circumferentially and folded in a less uniform manner. The stress of the bulge base induced initial stress on the column upon flattening of the bulge base. This in turn affected the responses and failure modes of the columns.

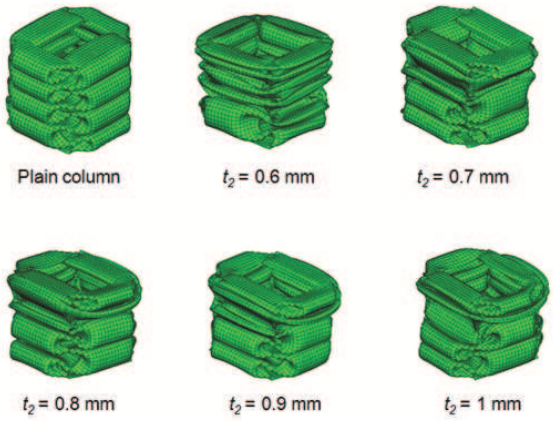

Fig. 8: Failure modes for the plain column and columns with different bulge base thicknesses under static loading

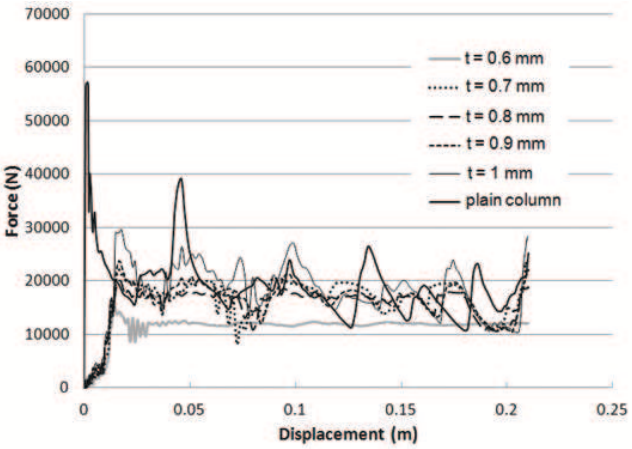

Fig. 7: Static responses for the plain column and columns with different bulge base thicknesses

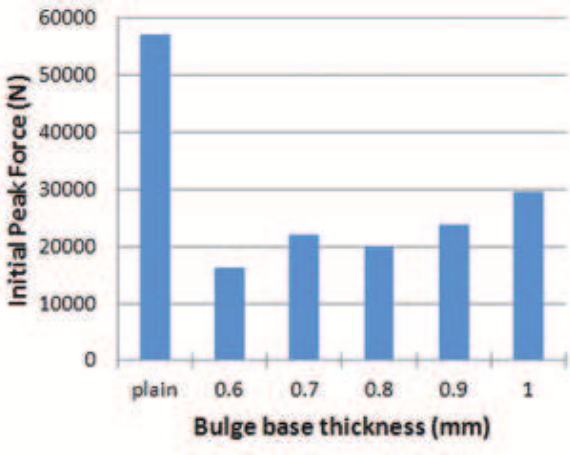

Fig. 9: Initial peak forces for the plain column and columns with different bulge base thickness under static loading

Figure 9 shows the initial peak forces for the plain column and columns with different bulge base thicknesses under static loading. The plain column has the highest initial peak force. Columns with bulge bases showed substantial reduction in initial peak force compared to the plain column. Column with bulge base of thickness 0.6 mm showed a reduction of 71.3% as compared to the plain column while the bulge base thickness of 1 mm reduced the initial peak force by 48.4%. Generally, reducing the bulge base thickness lowers the initial peak force.

5.2 Comparison between simulation results and analytical method

Figure 10 shows the comparison of initial peak force for both analytical method and simulations for columns with different bulge base thickness. Overall both methods yielded comparable results. Both analytical and simulation results showed gradual increase in initial peak force as the thickness of bulge base was increased. With the bulge base thickness of 0.0008 mm, there was a slight decrease in initial peak force. Further increasing the bulge base thickness to 0.001 mm gradually increased it again. The analytical method showed a linear increase in initial peak force with increasing bulge base thickness. It also showed higher values of initial peak force as compared to the simulation. This could be due to the approximations

i.e. deformed shape and uniform stress distribution that were made in the model.

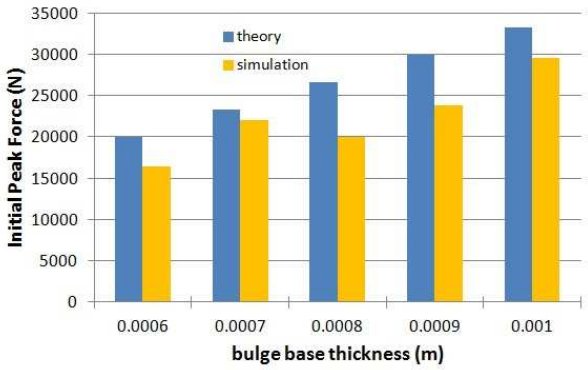

Fig. 10: Comparison of initial peak forces for both analytical method and simulations for columns with different bulge base thickness

6 Conclusions

The plain square column and columns with ellipsoidal bulge bases were subjected to static axial loading. Results showed that the bulge base significantly improved the crush performance of the square column especially in term of initial peak force. Generally, columns with bulge bases exhibited significant reduction in initial peak force. The column with a bulge base thickness of 0.6 mm had the lowest initial peak force, a reduction of 71.3% as compared to the plain column. Proposed analytical method compares favourably with the simulation results. The analytical method showed the same trend as the simulation results even though it slightly over predicted the initial peak forces. This work demonstrates that the crush performance of standard tubular structures can be improved by using an ellipsoidal bulge base as trigger mechanism. Further parametric study of the ellipsoidal bulge base configuration and experimental validation may be carried out to further optimize the design.

References

[1] Jones, N. (1997). Structural Impact. Cambridge University Press.
[2] Yu, T. X. and Lu, G. (2003). Energy absorption of structures and materials, Woodhead Publishing, Cambridge, United Kingdom.
[3] Olabi AG, Morris E, Hashmi MSJ (2007). Metallic tube type energy absorbers: A synopsis. Thin-walled Structures. **45**, pp 706-726.
[4] Alghamdi AAA. Collapsible impact energy absorbers: an overview (2001). Thin-walled Structures. **39**, pp 189-213.
[5] Alexander JM (1960). An approximate analysis of the collapse of thin cylindrical shelss under axial loading. Quarterly J Mechanics and Applied Mathematics. **13**, pp 10-15
[6] Mamalis AG, Manolakos DE, Saigal S, Viegelahn G, Johnson W (1996). Extensible plastic collapse of thin-walled frustaas energy absorbers. Int J Mech Sciences. **28**, pp 219-229.
[7] Chirwa EC (1993). Theoretical analysis of tapered thin-walled metal inverbucktube. Int J Mech Sciences. **35**, pp 325-351.
[8] Wierzbicki T, Abramovicz W (1983). On the crushing mechanics of thin walled structures. J Appl Mech. 50(4a): pp 727-734.
[9] Abramovicz W, Jones N (1984). Dynamic axial crushing of square tubes. Int J Impact Eng. **2**, pp 179-208.
[10] Abramovicz W, Jones N. Dynamic progressive buckling of circular and square tubes (1986). Int J Impact Eng. **4**, pp 243-270.
[11] Zhang X, Cheng G. A comparative study of energy absorption characteristics of foam filled and multi square columns (2007). Int J Impact Eng. **34**, pp 1739-1752.
[12] Daneshi GH and Hosseinipou SJ (2003). Grooves effect on crashworthiness characteristics of thin walled tubes under axial compression. Materials and Design. **23**, pp 611-617
[13] Zhang X, Cheng G, Zhang H (2009). Numerical investigation on a new type of energy absorbing structure based on free inversion of tubes. Int J Mech Sci. **51**, pp 64-76.
[14] Zhang XW, Su H, Yu TX (2009). Energy absorption of an axially crushed square tube with a buckling initiator. Int. J Impact Eng. **36**, pp 402-417.
[15] Zhang XW, Tian QD, Yu TX (2009). Axial crushing of circular tubes with buckling initiators. Thin-walled Struct. **47**, pp 788-797.
[16] Yamashita M, Kenmotsu H, Hattori T (2012). Dynamic axial compression of aluminium hollow tubes with hat cross-section and buckling initiator using inertia force during impact. Thin-walled Struct. **50**, pp 37-44.

M. A. Hassan is associate professor at the mechanical department, Faculty of Engineering, Assuit University, Egypt. Currently he is a visiting associate Professor at the Department of Engineering Design and Manufacture, Faculty of Engineering, UM. He has received his Master in 1997, Egypt. In 2002 He got his PhD in information and production science (forming technology), Kyoto Institute of technology, Japan. He has published more than 30 technical articles in the field of forming and micro forming, MEMS, Piezoelectric thin Films and heart mechanics.

Amir Radzi Ab. Ghani graduated in B. Eng. Mechanical from University of Liverpool in 1994. In 1995, he completed his M. Sc. Mechanical Systems Engineering from the same university. He has worked in SIRIM Bhd from 1995 till 2006 as an engineer and involved in the design and development of automotive and aerospace parts, machineries and transportation system. From 2006 to 2009, he worked as a lecturer in the Dept. of Engineering Design and Manufacture, Faculty of Engineering, University of Malaya. Currently he is attached to the Faculty of Mechanical Engineering, Universiti Teknologi MARA, Malaysia. His research interests are structural analysis, finite element analysis and structural crashworthiness. Most of his work deals with impact performance of metallic structures. He is a corporate member of The Institution of Engineers, Malaysia and a registered Professional Engineer with the Board of Engineers, Malaysia.

Zahari Taha received his BSc.Eng (Hons) degree in 1983 from Bath University, Bath, UK and his Ph.D. degree in 1987 from University of Wales, Cardiff, UK. He is currently a professor in the Department of Manufacturing Engineering, University Malaysia Pahang.

M. A. Hamdi received the B.Eng (Hons) degree from Imperial College London in UK and the M.Sc. degree from University of Manchester Institute of Science and Technology in UK, and the Ph.D. degree from Kyoto University in Japan. He is currently a professor in the Department of Engineering Design and Manufacture, Faculty of Engineering, University of Malaya. He is the author and coauthor of more than 100 publications in international journals.